Biomedical Optics EXPRESS

Zirconia dental implants degradation by confocal Raman microspectroscopy: analytical simulation and experiments

Nadia Djaker,[1,*] Claudine Wulfman,[2] Michaël Sadoun,[2] and Marc Lamy de la Chapelle[1]

[1] *Université Paris 13, Sorbonne Paris Cité, Laboratoire CSPBAT, CNRS (UMR 7244), 74 rue Marcel Cachin, 93017, Bobigny, France*

[2] *2URB2I-EA4462, Faculté de chirurgie dentaire, Université Paris Descartes, Sorbonne Paris cite, Paris, France*

[*] *nadia.djaker@univ-paris13.fr*

Abstract: Subsurface hydrothermal degradation of yttria stabilized tetragonal zirconia polycrystals (3Y-TZP) is presented. Evaluation of low temperature degradation (LTD) phase transformation induced by aging in 3Y-TZP is experimentally studied by Raman confocal microspectroscopy. A non-linear distribution of monoclinic volume fraction is determined in depth by using different pinhole sizes. A theoretical simulation is proposed based on the convolution of the excitation intensity profile and the Beer-Lambert law (optical properties of zirconia) to compare between experiment and theory. The calculated theoretical degradation curves matche closely to the experimental ones. Surface transformation (V_0) and transformation factor in depth (T) are obtained by comparing simulation and experience for each sample with nondestructive optical sectioning.

OCIS codes: (160.1435) Biomaterials; (170.1850) Dentistry; (170.5660) Raman spectroscopy; (180.1790) Confocal microscopy; (290.5860) Scattering, Raman.

References and links

1. M. Hisbergues, S. Vendeville, and P. Vendeville, "Zirconia: established facts and perspectives for a biomaterial in dental implantology," J. Biomed. Mater. Res. B **88B**(2), 519–529 (2009).
2. C. Piconi and G. Maccauro,"Zirconia as a ceramic biomaterial," Biomaterials **20**(1), 1–25 (1999).
3. H. Luthy, F. Filser, O. Loeffel, M. Schumacher, L. J. Gauckler, and C. H. F. Hammerle,"Strength and reliability of four-unit all-ceramic posterior bridges," Dent. Mater. **21**(10), 930–937 (2005).
4. J. S. Schley, N. Heussen, S. Reich, J. Fischer, K. Haselhuhn, and S. Wolfart, "Survival probability of zirconia-based fixed dental prostheses up to 5 yr: a systematic review of the literature," Eur. J. Oral Sci. **118**(5), 443–450 (2010).
5. K. Kobayashi, H. Kuwajima, and T. Masaki, "Phase-change and mechanical properties of ZrO2-Y2O3 solid electrolyte after aging," Solid State Ionics **3-4**(AUG), 489–493 (1981).
6. S. S. Brown, D. D. Green, G. Pezzotti, T. K. Donaldson, and I. C. Clarke, "Possible triggers for phase transformation in zirconia hip balls," J. Biomed. Mater. Res. B **85B**(2), 444–452 (2008).
7. J. A. Munoz-Tabares, E. Jimenez-Pique, and M. Anglada, "Subsurface evaluation of hydrothermal degradation of zirconia," Acta Mater. **59**(2), 473–484 (2011).
8. H. Toraya, M. Yoshimura, and S. Somiya, "Quantitative-analysis of monoclicnic-stabilized cubic ZrO2 systems by X-ray-diffraction," J. Am. Ceram. Soc. **67**(9), C183–C184 (1984).
9. S. Deville, L. Gremillard, J. Chevalier, and G. Fantozzi, "A critical comparison of methods for the determination of the aging sensitivity in biomedical grade yttria-stabilized zirconia," J. Biomed. Mater. Res. B **72B**(2), 239–245 (2005).

#185242 - $15.00 USD Received 11 Feb 2013; revised 15 Mar 2013; accepted 27 Mar 2013; published 12 Apr 2013

10. C. Wulfman, N. Djaker, N. Dupont, D. Ruse, M. Sadoun, and M. Lamy de la Chapelle, "Raman spectroscopy evaluation of subsurface hydrothermal degradation of zirconia," J. Am. Ceram. Soc. **95**(7), 2347–2351 (2012).
11. C. Wulfman, M. Sadoun, and M. Lamy de la Chapelle, "Interest of Raman spectroscopy for the study of dental material: the zirconia material example," IRBM **31**(5-6), 257–262 (2010).
12. D. Casellas, F. L. Cumbrera, F. Sanchez-Bajo, W. Forsling, L. Llanes, and M. Anglada, "On the transformation toughening of Y-ZrO2 ceramics with mixed Y-TZP/PSZ microstructures," J. Am. Ceram. Soc. **21**(6), 765–777 (2001).
13. J. A. Munoz-Tabares, and M. J. Anglada, "Quantitative analysis of monoclinic phase in 3Y-TZP by Raman spectroscopy," J. Am. Ceram. Soc. **93**(6), 1790–1795 (2010).
14. J. Barbillat, P. Dhamelincourt, M. Delhaye, and E. Dasilva, "Raman confocal microprobing, imaging and fiber-optic remote sensing: a further step in molecular analysis," J. Raman Spectrosc. **25**(1), 3–11 (1994).
15. G. Pezzotti, and A. A. Porporati, "Raman spectroscopic analysis of phase-transformation and stress patterns in zirconia hip joints," J. Biomed. Opt. **9**(2), 372–384 (2004).
16. V. Presser, M. Keuper, C. Berthold, and K. G. Nickel, "Experimental determination of the Raman sampling depth in zirconia ceramics," Appl. Spectrosc. **63**(11), 1288–1292 (2009).
17. G. Pezzotti, K. Yamada, A. A. Porporati, M. Kuntz, and K. Yamamoto, "Fracture toughness analysis of advanced ceramic composite for hip prosthesis," J. Am. Ceram. Soc. **92**(8), 1817–1822 (2009).
18. A. Gallardo, S. Spells, R. Navarro, and H. Reinecke, "Confocal Raman microscopy: how to correct depth profiles considering diffraction and refraction effects," J. Raman Spectrosc. **38**(7), 880–884 (2007).
19. A. M. Macdonald and A. S. Vaughan, "Numerical simulations of confocal Raman spectroscopic depth profiles of materials: a photon scattering approach," J. Raman Spectrosc. **38**(5), 584–592 (2007).
20. S. L. Jacques, B. Wang, and R. Samatham, "Reflectance confocal microscopy of optical phantoms," Biomed. Opt. Express **3**(6), 1162–1172 (2012).
21. W. Song, J. Lee, and H. S. Kwon, "Enhancement of imaging depth of two-photon microscopy using pinholes: analytical simulation and experiments," Opt. Express **20**(18), 20605–20622 (2012).
22. http://www.zeiss.de/C1256D18002CC306/0/F99A7F3E8944EEE3C1256E5C0045F68B/$file/60-1-0030_confocal-principles.pdf
23. J. Salem and D. Zhu, *Ceramic Coatings and Interfaces II*, U. Schulz and H. T. Lin eds. (Wiley-Interscience, 2007).
24. D. Wang, Y. Chen, and J. T. C. Liu, "A liquid optical phantom with tissue-like heterogeneities for confocal microscopy," Biomed. Opt. Express **3**(12), 3153–3160 (2012).

1. Introduction

Zirconia is among the most biocompatible materials widely used in medical applications [1, 2]. Since seventies, zirconia has known several applications as implants, but recently in the dentistry domain for crowns and fixed partial dentures [3]. Especially, Tetragonal zirconia doped with 3 % mol of yttria (3Y-TZP) is used because of its high strength and fracture toughness [4]. Zirconia crystal structure knows three phases depending on temperature: the monoclinic phase (m), the tetragonal phase (t) and the cubic phase (c). During aging of 3Y-TZP dental implants tetragonal to monoclinic phase transformation occurs due to the environment humidity. In this phenomenon known as low temperature degradation (LTD), the transformation from tetragonal to monoclinic phase begins at the surface and spreads inside the implant causing microcracks and mechanical properties degradation. The hydrothermal degradation was reported first by Kobayashi et al [5] and was widely documented in previous works [6, 7]. Artificial LTD on zirconia is studied to predict implants degradation by aging. In this case, monoclinic phase fraction is measured as a function of temperature and time of humidity exposure. Several techniques for zirconia transformation study were reported: transmission electron microscopy, X-ray diffraction, optical interferometry and AFM [8, 9]. But, they are limited to the surface analysis or involve the sample section. Raman microspectroscopy is an alternative technique for a local analysis of tetragonal to monoclinic phase transformation [10, 11]. Quantitative analysis are obtained from tetragonal and monoclinic phases spectra, by measuring the Raman band intensity of each phase, which depends directly on their relative concentration. Different ways of quantification of monoclinic/tetragonal proportions in zirconia samples was proposed using Raman spectroscopy always on cross-sections [12, 13]. Raman confocal microspectroscopy (RCMS) offers a supplementary advantage in zirconia transformation analysis. Its high axial

#185242 - $15.00 USD Received 11 Feb 2013; revised 15 Mar 2013; accepted 27 Mar 2013; published 12 Apr 2013

resolution (2 μm) permits to probe samples with a resolution depending on the zirconia optical properties (absorption and scattering) by using optically conjugate pinhole diaphragms [14]. The depth profile has been calibrated by using optical properties of excitation wavelength and objective numerical aperture [15, 16]. However, few is reported on probing tetragonal to monoclinic phase transformation in depth because of sample preparation (sample sectioning) [17]. For in-depth studies by RCMS technique, the optical sectioning is more suitable for transparent samples. Recently, correction of depth profiles considering diffraction and refraction in polymers was reported [18, 19]. In this study, RCMS is used to probe tetragonal to monoclinic phase transformation of different aging times of 3Y-TZP samples without any sample sectioning by using different pinhole sizes. A theoretical model is proposed based on the optical properties of the excitation laser (wavelength), the objective characteristics (numerical aperture, magnification) and the zirconia optical properties (refraction index, absorption and scattering coefficients). Experimental and theoretical zirconia transformation curves are compared and transformation factors are provided by using a totally non-destructive method for in-depth analysis.

2. Materials and methods

Experimental zirconia transformation curves were obtained on (20x4x2) mm^3 specimens with a pure tetragonal crystalline structure assessed before aging by Raman spectroscopy. The samples were exposed to in vitro aging in Ringer solution at 130^{o}C and 0.6 MPa for 25h and 90h. Raman spectra of transformed zirconia were recorded using a Labram Raman spectrometer (Horiba Jobin Yvon, Kyoto, Japan). The excitation laser was a HeNe laser (633 nm) with 1 mW power. The Raman spectrometer was combined to a confocal microscope (Olympus LX71).

In this study, an objective 10x, NA 0.25 was used. Considering the refraction index of zirconia (n=2.2), the effective numerical aperture (NA_{eff}) as described in [20] is NA/n=0.11. This gives an axial resolution due to the refractive effect of 70μm ($FWHM_z = 1.4\lambda/NA_{eff}^2$).

Combining the objective with gradually enlarged confocal pinhole apertures, from 30 to 300 μm, allows the control of the probe size and thus of the collection depth (z_{exp}). Pinhole function as rejecting out-of focus signals, enables thin optical sectionning within thick samples [21].

The principle of the confocal microprobe method is illustrated in Fig. 1. Pinhole size variation leads to different optical slice sizes described theoretically in transparent media by Eq. (1) [22]:

$$z_{opt} = \sqrt{\left(\frac{0.88\lambda_{Raman}}{1-\sqrt{1-NA^2}}\right)^2 + \left(\frac{\sqrt{2}PH^2}{NA}\right)^2} \quad (1)$$

With: λ_{Raman}, the emitted Raman wavelength of zirconia at the vibrational frequency of 256 cm^{-1} ($\lambda_{Raman} = 643nm$), PH, the object-side pinhole diameter [μm] and NA, the numerical aperture of the objective.

Moreover, zirconia is also a highly scattering medium whereas the absorption coefficient of 3Y-TZP can be neglected ($\mu_a = 0.135cm^{-1}$), in front of the reduced scattering coefficient ($\mu_s^{'} = 100cm^{-1}$ from [23]). The optical slice described previously in transparent media should then be modified according to this scattering effect. The study of in-depth variation in scattering media as phantoms was reported [20, 24]. To determine this scattering effect, a calibration of the optical slice sizes is necessary depending on the pinhole size. In case of zirconia, the calibration of collection depth was conducted on a highly-polished knife-shaped specimen as reported by the authors and based on the protocol previously described in [10]. In this study, we have compared the theoretical and experimental optical depths obtained in zirconia.

Figure 2 (left) shows the calculated axial optical slices (z_{opt}) in non-scattering media given by Eq. (1) and the measured experimental depths by knife-edge technique obtained for differ-

#185242 - $15.00 USD Received 11 Feb 2013; revised 15 Mar 2013; accepted 27 Mar 2013; published 12 Apr 2013

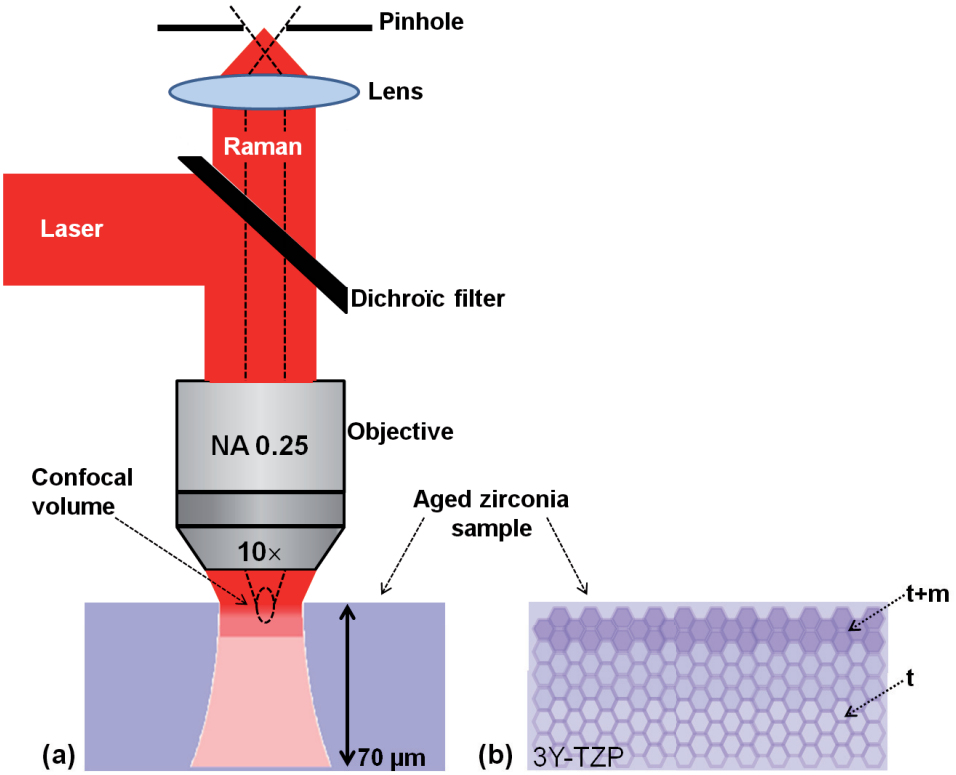

Fig. 1. Schematic presentation of confocal detection principal in the confocal Raman micro-spectroscopy.

ent pinhole sizes. The ratio between experimental (z_{exp}) and theoretical (z_{opt}) optical slices is due to the scattering effect. In Fig. 2 (right), we see that this ratio is fitted by an exponential law as Beer-Lambert law which describes this scattering effect ($I(z) = I_0 e^{-\mu z}$ where I(z) is the intensity axial profile). Since the absorption is neglected in zirconia, only the scattering coefficient ($\mu_s^{'} = 0.01 \mu m^{-1}$) is present. A factor of 2 is added in the fit curve due to the fact that, the scattering is considered twice: one time for excitation laser scattering and a second time for Raman diffusion scattering.

After depth penetration calibration, Raman spectra were collected from three randomly selected points on the surface of each aged specimen. Raman spectra were measured in 22 probes following the same protocol. The purity of the tetragonal phase was assessed in the control samples. Close to 800 spectra were collected and analyzed. Raman peak positions and intensities were obtained by fitting the Raman spectra with Lorentzian curves. From each spectrum, the monoclinic volume fraction V_{fm} was calculated. Noise in Raman spectra was very low and the bands picks fittings give errors bars in V_{fm} calculations which were presented on the experimental graphs.

The spectra of the tetragonal and of the monoclinic phases are sufficiently different to enable qualitative analysis. Each structure exhibits specific features that can be assigned to actual spectral signature of the studied phases. In the tetragonal phase, the most characteristic bands are a sharp band at 142 cm^{-1} and a broader one at 256 cm^{-1}, whereas, in the monoclinic phase, a doublet is seen at 178 and 190 cm^{-1}. Raman spectra of aged zirconia were reported by the authors in [10]. The zirconia degradation occurs during the tetragonal to monoclinic transfor-

#185242 - $15.00 USD Received 11 Feb 2013; revised 15 Mar 2013; accepted 27 Mar 2013; published 12 Apr 2013

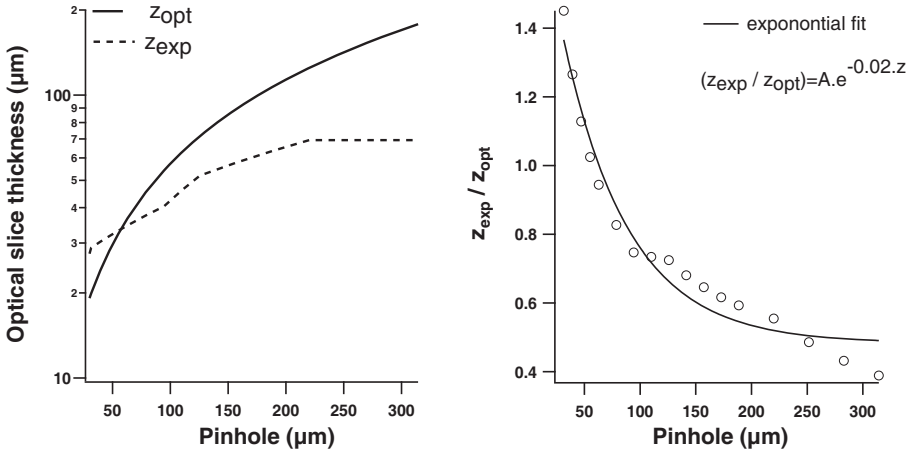

Fig. 2. Calculated optical slice thickness given by the optical objective and measured axial depths in zirconia for each pinhole size (left) Ratio between calculated and measured depths.

mation, which is estimated by calculating the monoclinic volume fraction, V_{fm}, using Eq. (2) [10, 11]. The calibration constant of 0.33 included in the ratio between the intensities of the monoclinic and tetragonal peaks taken in this work was widely discussed [13], and used to calculate the monoclinic fraction volume:

$$V_{fm} = \frac{I_m^{178} + I_m^{189}}{0.33\left(I_t^{145} + I_t^{256}\right) + I_m^{178} + I_m^{189}} \tag{2}$$

Where I_m and I_t are the intensities of the Raman peaks of the monoclinic and tetragonal phases and 0.33 is the correction factor for the difference of the scattering cross section between the selected peaks of the monoclinic and tetragonal phases. Since the transformation curves (see Fig. 3) are recorded in depth without mechanically cutting the samples but with optical sectioning, their profile is modified by the optical properties of excitation laser (wavelength), the objective used (NA) and the zirconia optical properties (refraction index, absorption and scattering) as explained below.

3. Results and discussion

Theoretically, the monoclinic fraction measured depends on the laser intensity Gaussian profile ($e^{-\frac{z^2}{0.4D_z^2}}$ with D_z, the axial resolution of the objective), the optical properties of zirconia (described by Beer-Lambert law: $e^{-\mu_s' z}$) and a sigmoid model describing the theoretical monoclinic volume fraction F(z) in depth as proposed by [7] (see Fig. 4 (left)). The optically modified fraction profile includes the contribution of optical parameters (excitation and beer-Lambert law with zirconia optical parameters) to the real transformation profile described in Eq. (2). This optically modified monoclinic fraction profile OF(z) is then described by Eq. (3):

$$OF(z) = e^{-\frac{z^2}{0.4D_z^2}} \times e^{-\mu z} \times \left(V_0 \times \frac{1 + e^{-T.z_0}}{1 + e^{T(z - z_0)}}\right) \tag{3}$$

Where V_0 is the monoclinic volume fraction on the surface ($z = 0$), T is the transformation factor in depth and Z_0 is the abscissa of the curve inflection point.

#185242 - $15.00 USD Received 11 Feb 2013; revised 15 Mar 2013; accepted 27 Mar 2013; published 12 Apr 2013

A simulation program based on Eq. (3) was developed using Igor software (WaveMetrics, Portland, USA). This program provide a theoretical curve, matching closely to the experimental averaged monoclinic fraction shown in Fig. 3 by variating the parameters: V_0, T and z_0.

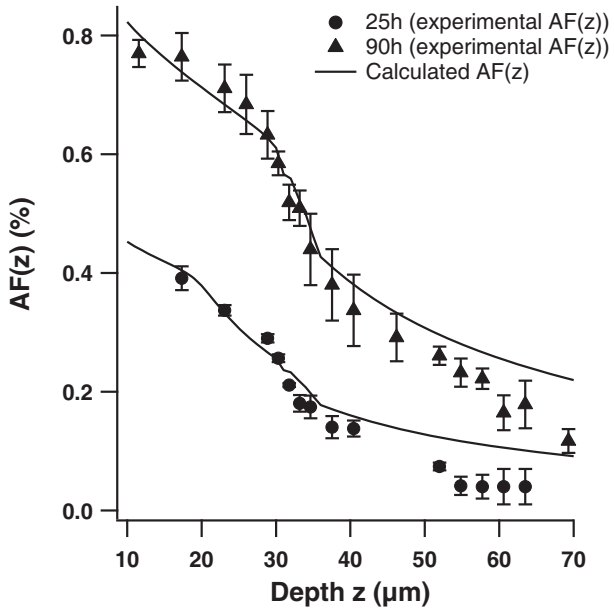

Fig. 3. Measured and calculated averaged monoclinical fraction in depth.

In fact, these experimental curves represent the average monoclinic fraction (AF) measured from the surface down to the depth z for each pinhole size. Indeed, as it was shown, the optical slices represent the collected signal from the surface down to optical depths (z) that are collected by each pinhole size. Thus, the average monoclinic fraction (AF) corresponds to the ratio between the collected monoclinic fraction (OF) and the optical slice thickness (z_{exp}). Theoretically, the experimental design with progressive enlargement of pinhole diameter enables the measurement of monoclinic volume fraction in increasing thickness of material AF (z), which can be written:

$$AF\,(z) = \frac{\int_0^z OF\,(z)\,dz}{z_{exp}} \tag{4}$$

The average fraction (AF) is the theoretical description of the measured transformation profiles (V_{fm} calculated using Eq. (2)) by confocal Raman micro-spectroscopy for each optical slice defined for each pinhole size. Figure 3 shows the experimental zirconia transformation AF(z) for two aged times. These experimental curves are compared to the theoretical averaged monoclinic volume fraction inside the collected depth AF(z) obtained by simulation program. Thus, to have the closest profiles, the simulation program fixes the transformation parameters V_0, T and z_0, such as T=1.1 μm^{-1} for both aging times, whereas, $z_0 = 30\mu m$ and $V_0 = 78\%$ for 90h and $z_0 = 20\mu m$ and $V_0 = 45\%$ for 25h aging time.

This means that the real transformation profile (F(z)) can be determined precisely directly from the simulation of the AF(z) curve and the fit of the experimental AF(z) curve. Figure 4 shows the result of the calculated monoclinic fraction axial profile for the theoretical monoclinic fraction (F(z)) and the optically modified monoclinic fraction (OF(z)) using Eq. (3) depending on pinhole sizes. The transformation parameters, V_0, T and z_0 have been fixed by the simulation

#185242 - $15.00 USD Received 11 Feb 2013; revised 15 Mar 2013; accepted 27 Mar 2013; published 12 Apr 2013

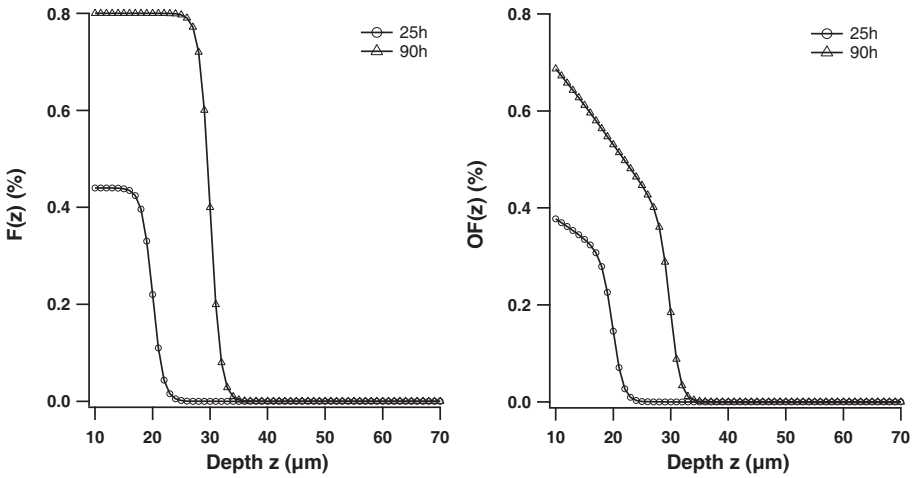

Fig. 4. Calculated monoclinic fraction in depth for two different aging times.

program. In this work, the theoretical monoclinic volume fraction curves (F(z)) are calculated without any sample cross section and are very close to profile curves obtained by sample cut reported before [7]. F(z) is integrated and averaged in the confocal depth to obtain finally the calculated averaged monoclinic fraction (AF(z)), which corresponds closely to the experimental one measured by confocal Raman microspectroscopy. The transformation parameters (V_0, T and z_0) are obtained for zirconia hydrothermal degradation in depth which allows the prediction of LTD for different other aging times.

4. Conclusion

In this study, the evolution of transformation (LTD) of 3Y-TZP is simulated and compared with experimentally measured LTD by confocal Raman micro-spectroscopy. The experimental method and the simulation model that we have proposed allow optical sectioning in depth by using different pinhole sizes to avoid any mechanical sectioning. The optical sectioning microscope was used to study a highly scattering media as zirconia used in dental crowns. The developped simulation program allows depths corrections and LTD factors estimation. This leads to the prediction of real transformation factors and profiles for any aging times without any mechanical sectionning which could induce some additional degradations. In addition, this simulation will be useful to model hydrothermal degradation in different dental materials based on zirconia using Raman confocal micro-spectroscopy.

#185242 - $15.00 USD Received 11 Feb 2013; revised 15 Mar 2013; accepted 27 Mar 2013; published 12 Apr 2013